Supporting Information

for

Fatty Acid-Based Polymeric Micelles to Ameliorate Amyloidogenic Disorders

Avisek Bera,[a] Debangana Mukhopadhyay,[b] Kalyan Goswami,[c] Pooja Ghosh,[a,*] Rumi De[b,*] and Priyadarsi De[a,*]

[a]Polymer Research Centre and Centre for Advanced Functional Materials, Department of Chemical Sciences, Indian Institute of Science Education and Research Kolkata, Mohanpur - 741246, Nadia, West Bengal, India.

[b]Department of Physical Sciences, Indian Institute of Science Education and Research Kolkata, Mohanpur - 741246, Nadia, West Bengal, India.

[c]Department of Biochemistry, All India Institute of Medical Sciences (AIIMS), Kalyani, Basantapur, NH-34 connector, Kalyani - 741245, Nadia, West Bengal, India.

*Corresponding Authors: E-mails: pgk89@iiserkol.ac.in; rumi.de@iiserkol.ac.in; p_de@iiserkol.ac.in

Experimental section

RAFT polymerization of PEGMA. Poly(polyethylene glycol methyl ether methacrylate) homopolymer ($PPEGMA_{300}$) was synthesized by RAFT polymerization technique, as reported earlier.[1] For the synthesis of the homopolymer, $PEGMA_{300}$ (2 g, 6.66 mmol), CTP (46.6 mg, 0.16 mmol), AIBN (5.47 mg, 0.33 μmol) and DMF were taken in 20 mL septa sealed polymerization reaction vial at a feed ratio of $[PEGMA_{300}]/[CTP]/[AIBN]$ = 40/1/0.2. The reaction vial was then purged with dry N_2 for 10 min and kept on a reaction block at 70 °C under constant stirring. After 6 h, the reaction was stopped by cooling in an ice bath followed by exposure to air. Finally, the resulting polymer was purified by precipitation in acetone/hexanes mixture 4-5 times and allowed to dry under vacuum for 12 h at 45 °C.

Similarly, $PPEGMA_{475}$ homopolymer was synthesized at a feed ratio of $[PEGMA_{475}]/[CTP]/[AIBN] = 40/1/0.2$ using RAFT polymerization technique.

Synthesis of block copolymers. Fatty acid-based block copolymers were synthesized by using RAFT polymerization technique. Typically, fatty acid-based monomers FAMA, $PPEGMA_{300}$ as a macro-CTA, and AIBN as an initiator were placed in 20 mL septa sealed polymerization vial at a feed ratio of [FAMA]/[PPEGMA]/[AIBN] = 10/1/0.2 in THF solvent followed by purging with dry N_2 for 15 min and placed in a preheated reaction chamber at 60 °C under continuous stirring. The polymerization reaction was then continued up to 6 h, and after 6 h the reaction was quenched by cooling the vial in an ice-water bath and exposed to air. Then, the purification of the resultant polymers was carried out by dialysis against MeOH (MWCO membrane of 2000 Da). During dialysis, MeOH was changed in a period of 3 to 8 h for at least 8 times. Finally, the polymeric solutions obtained were allowed to evaporate under a rotary evaporator and dried under vacuum at 45 °C for 12 h. Similarly, another block copolymer $PPEGMA_{475}$-*b*-PSAMA was synthesized using a higher molecular weight of PEG side-chain in the $PPEGMA_{475}$ macro-CTA.

Synthesis of insulin fibrils in the absence and presence of FABC micelles. *In vitro* insulin fibrils were synthesized as described in a previous literature report.[3] Insulin fibrils were obtained by suspending native insulin directly in HCl solution (10 mM; pH 2.0) to 1 mg/mL concentration followed by incubation at 65 °C for 24 h under constant stirring at 250 rpm. To confirm the effect of the **FABC** micelles on insulin fibrillation process, different types of **FABC** micelles (1 mg/mL) were added into the native insulin solution keeping other conditions same as discussed above and incubated for a period of 24 h.

Determination of critical aggregation concentration (CAC). The CAC values of the synthesized block copolymers were evaluated by fluorescence spectrophotometer where pyrene was taken as a hydrophobic fluorescent probe.[2,3] To determine the CAC values, 6 μL

of pyrene solution in acetone was taken from stock and added separately to the different glass vials containing different concentrations of aqueous polymeric solution, and the final concentration of pyrene was fixed at 10^{-7} mol/L in each vial. The vials were then kept open for 6 h to evaporate the acetone completely. The fluorescence emission intensities were then measured at an excitation wavelength of 337 nm, and the slit width was fixed at 3 nm. The ratio of the fluorescence emission intensity of the first and third vibration peaks (I_{393}/I_{373}) was plotted against the logarithm of the polymer concentration. The intersection point obtained from the plot corresponds to the CAC value.

Thioflavin T (ThT)-based fluorescence assay. ThT-based fluorescence assay was conducted for *in vitro* quantification and identification of insulin fibrils.[4] In this experiment, 24 μL of aliquots from each sample set were taken and mixed with 10 μL of ThT (1 mM stock solution) in 50 mM Tris-HCl buffer (pH 8.0) to make the final concentrations of protein and ThT at 2 and 5 μM, respectively. After 10 min of incubation of the samples, the ThT fluorescence emission intensity of the samples was measured at 485 nm upon excitation at 450 nm, keeping the slit width fixed at 5 nm for both excitation and emission, and the integration time was set at 0.3 s.

Similarly, ThT-based kinetic experiments were carried out for a period of 24 h by taking out aliquots from each sample set at different fixed time intervals for 0 to 24 h. The samples were then mixed with ThT in 50 mM Tris-HCl buffer (pH 8.0) followed by incubation for 5 min, and ThT emission spectra were acquired using a Horiba JobinYvon Fluoromax-3 spectrophotometer. The kinetic data obtained from the ThT-based kinetic results were fitted using a sigmoidal equation (1) as follows, and the different kinetic parameters such as lag phase time (t_{lag}), and rate constant (k) were determined from the equation (1).

$$Y = Y_0 + \frac{Y_{max}}{1 - exp\frac{t - t_{1/2}}{k}} \qquad (1)$$

where Y symbolizes the ThT emission intensity measured after an incubation period t; Y_0 and Y_{max} signify the ThT emission intensity of the initial insulin monomers and final insulin fibrils, respectively; $t_{1/2}$ is the time needed to reach the half-maximal emission intensity. Besides, the t_{lag} of the fibrillation pathway was calculated by using the following equation (2):

$$t_{lag} = t_{1/2} - \frac{2}{k} \qquad (2)$$

Turbidity assay. Turbidity-based measurements were performed to assess the extent of aggregation of insulin fibrils in the absence and presence of **FABC** micelles by measuring the absorbances of the samples at 350 nm using UV-Vis spectrophotometer.[5] To perform this assay, 5 μM concentration of samples were prepared in Tris-HCl buffer (50 mM, pH 8.0), and then the absorbance values were recorded at a particular wavelength of 350 nm using 1 cm path length of quartz cuvette.

Intrinsic fluorescence measurements. Intrinsic fluorescence measurements were conducted to monitor the local environmental changes around the hydrophobic Tyrosine (Tyr) amino acid residues. For this study, 60 μL of sample from each stock solution of native insulin, insulin fibrils, and **FABC** micelles treated insulin fibrils were diluted with 50 mM Tris-HCl buffer (pH 8.0) to make the final concentrations of each sample at 5 μM. The Tyr fluorescence emission intensity of the samples was then measured at 305 nm keeping the excitation wavelength fixed at 276 nm, slit width 5 nm, and integration time 0.2 s.

Nile red (NR) fluorescence assay. To perform NR fluorescence assay, at first, NR stock solution (1 mM) was prepared in methanol. Then, IF in the absence and presence of **FABC** micelles were incubated with NR (1 mM) for 30 min in the dark, and the final concentration of sample and NR solution were maintained at 2.5 and 10 μM, respectively. After the incubation period, the fluorescence emission spectra of all the samples were measured in the region of 540-

800 nm by keeping the excitation wavelength fixed at 530 nm. The other parameters like slit width and integration time were set at 5 nm and 0.3 sec, respectively.

Time-resolved fluorescence measurements. The time-correlated single-photon counting (TCSPC) method was employed to determine the fluorescence lifetimes of the samples by using a picoseconds spectrofluorimeter of Horiba Jobin Yvon IBH. The instrument was equipped with a FluoroHub single photon counting controller and a FC-MCP-50SC MCP-PMT detection unit. A 408 nm diode laser with a temporal resolution of <200 ps was used as the excitation source. The data were collected using TCSPC method, and the analysis was done by fitting the data using the IBH DAS6 (version 2.2) software by the nonlinear least-squares iterative re-convolution method. The average lifetimes $<\tau>$ were calculated using the following equation (3).[6] The *B* values indicate the respective pre-exponential factors.

$$<\tau>=\frac{\sum B_i\tau_i^2}{\sum B_i\tau_i} \qquad (3)$$

Fluorescence lifetime imaging microscopy (FLIM). Fluorescence lifetime imaging microscopy measurements were carried out with a confocal laser scanning microscope (Axio Observer A1) from Zeiss, equipped with a DCS-120 system from Becker & Hickl (BH) GmbH using 40× objectives. The sample excitation was done using a picosecond diode laser (BDL-488-SMC, BH) with λ_{ex} = 405 nm, and a long pass filter (HQ495LP) was used to block the excitation source. A narrow band-pass filter of 525-550 nm (HQ525/50) was utilized for monitoring the emission. The scanning was regulated by a BH GVD-120 scan controller. The BH HPM-100-40 hybrid detector module in the DCS-120 system was controlled by DCC-100 software. For our experiment, we have used 4-(dicyanomethylene)-2-methyl-6-(4-dimethylaminostyryl)-4H-pyran (DCM) dye as a fluorescence marker. Briefly, 1 mM stock DCM solution was prepared in methanol. Then, 5 µL of samples (1 mg/mL) was mixed with 10 µL of DCM (1 mM) and allowed to incubate for 10 min. Next, one drop of the sample was

placed on a glass slide and covered with a coverslip, and images were captured under the microscope and analyzed using SPCImage software.

Transmission electron microscopy (TEM) analysis. TEM analysis was performed to observe the morphology of **FABC** micelles as well as to verify the changes in morphology and fibrillar growth of IF in the presence of **FABC** micelles. Briefly, 5 µL of IF and **FABC** micellar solution was taken from the stock sample set and diluted with 50 mM Tris-HCl buffer (pH 8.0) so that the concentration of each sample was fixed at 50 µg/mL. On the other hand, during the analysis of morphology of **FABC** micelles, the concentration of micelles was fixed at 1 mg/mL. After preparing the samples, a drop of the sample was placed on a carbon-coated 300 mesh TEM grid and air dried. TEM images were then collected using JEOL JEM-2100F electron microscope.

Field emission scanning electron microscopy (FESEM). FESEM was used to analysis the change in the extent of fibrillar growth of IF in the presence of **FABC** micelles. For FESEM analysis, 100 µg/mL concentration of each samples was mounted on a cleaned coverslip. The coverslip was then allowed to dry in air initially and then placed in a vacuum desiccator. Before taking the images, the samples were coated with gold, and the images were then viewed under a Carl Zeiss Sigma instrument.

Dynamic light scattering (DLS) measurements. The change in average sizes of IF in the presence of **FABC** micelles was monitored by DLS measurements. For this experiment, samples (final concentration: 0.5 mg/mL) were diluted with Milli-Q water, and then the average sizes were measured using a Malvern Nano ZS instrument.

Circular dichroism (CD) analysis. In order to monitor the changes in secondary structures of IF in the presence of **FABC** micelles, CD technique was employed.[7] CD spectra were acquired in the wavelength range of 190-240 nm in 0.1 cm pathlength of cuvette at 25 °C. The bandwidth and response time were set at 1.0 nm and 4 s, respectively, and the scanning

speed was maintained at 50 nm/min. Each spectrum was collected three times, and then the average spectra were taken. DICHROWEB, an online server, was used to evaluate the different secondary structural contents of IF in the absence and presence of **FABC** micelles.

Hemolysis study. To explore the impact of **FABC** micelles on IF induced cytotoxicity and membrane disruption, hemolysis study was conducted.[8,9] For the hemolytic assay, at first, blood from goat was collected from local market and was allowed to centrifuge at 3500 rpm for 15 min. Then red blood cells (RBCs) were separated from plasma and buffy coat by continuously washing (× 5) with phosphate buffered saline (pH 7.4). Next, the RBC suspension (1% hematocrit) was incubated with IF in the absence and presence of **FABC** micelles at 37 °C for 40 min. After 40 min, the samples were again centrifuged at 3500 rpm for 15 min, and the absorbance value was recorded at 540 nm, which is actually the absorption maxima of haemoglobin. Hemolysis of RBCs with 1% Triton X-100 was considered as 100%, and the hemolytic rate of IF in the absence and presence of FAMA micelles was calculated with respect to the hemolysis of Triton X-100.

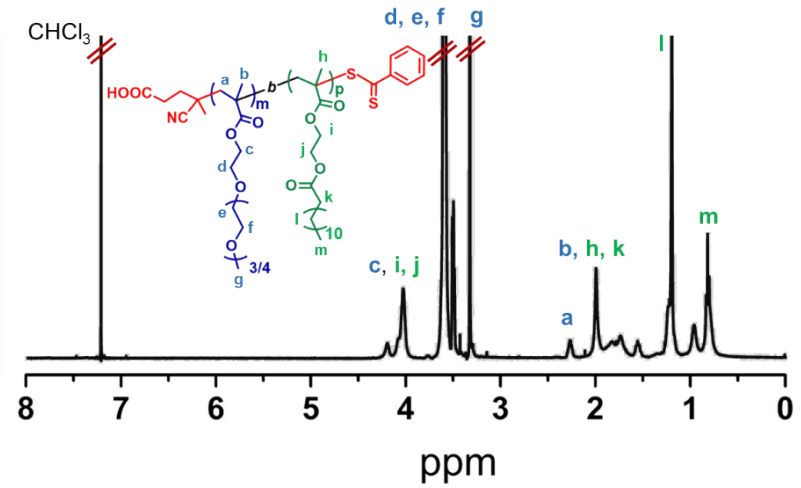

Fig. S1 ^{1}H NMR spectrum of PPEGMA$_{300}$-*b*-PMAMA in $CDCl_3$.

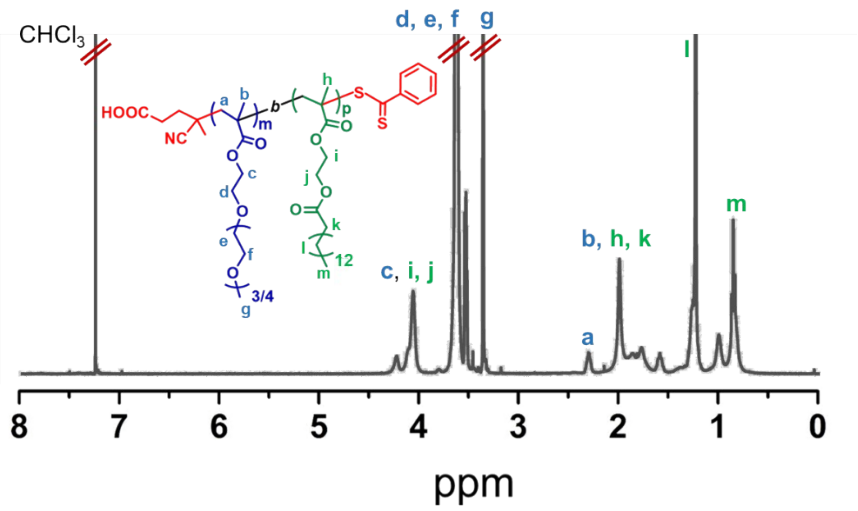

Fig. S2 ^{1}H NMR spectrum of PPEGMA$_{300}$-*b*-PPAMA in $CDCl_3$.

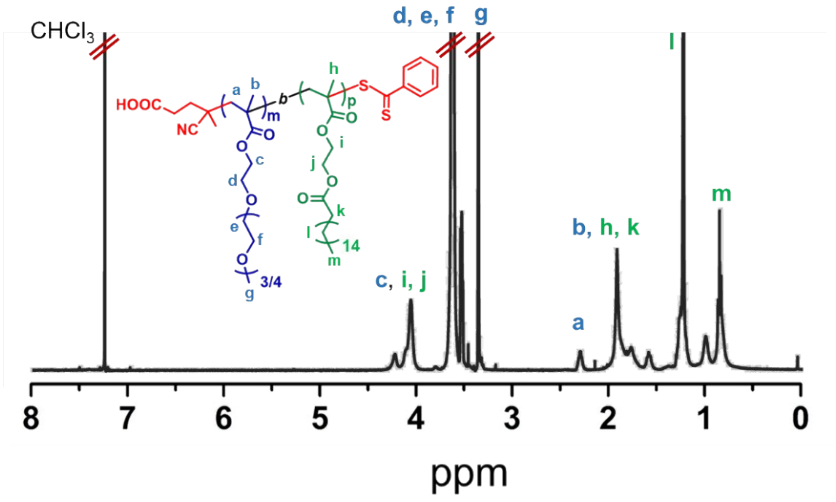

Fig. S3 ^{1}H NMR spectrum of PPEGMA$_{300}$-*b*-PSAMA in $CDCl_3$.

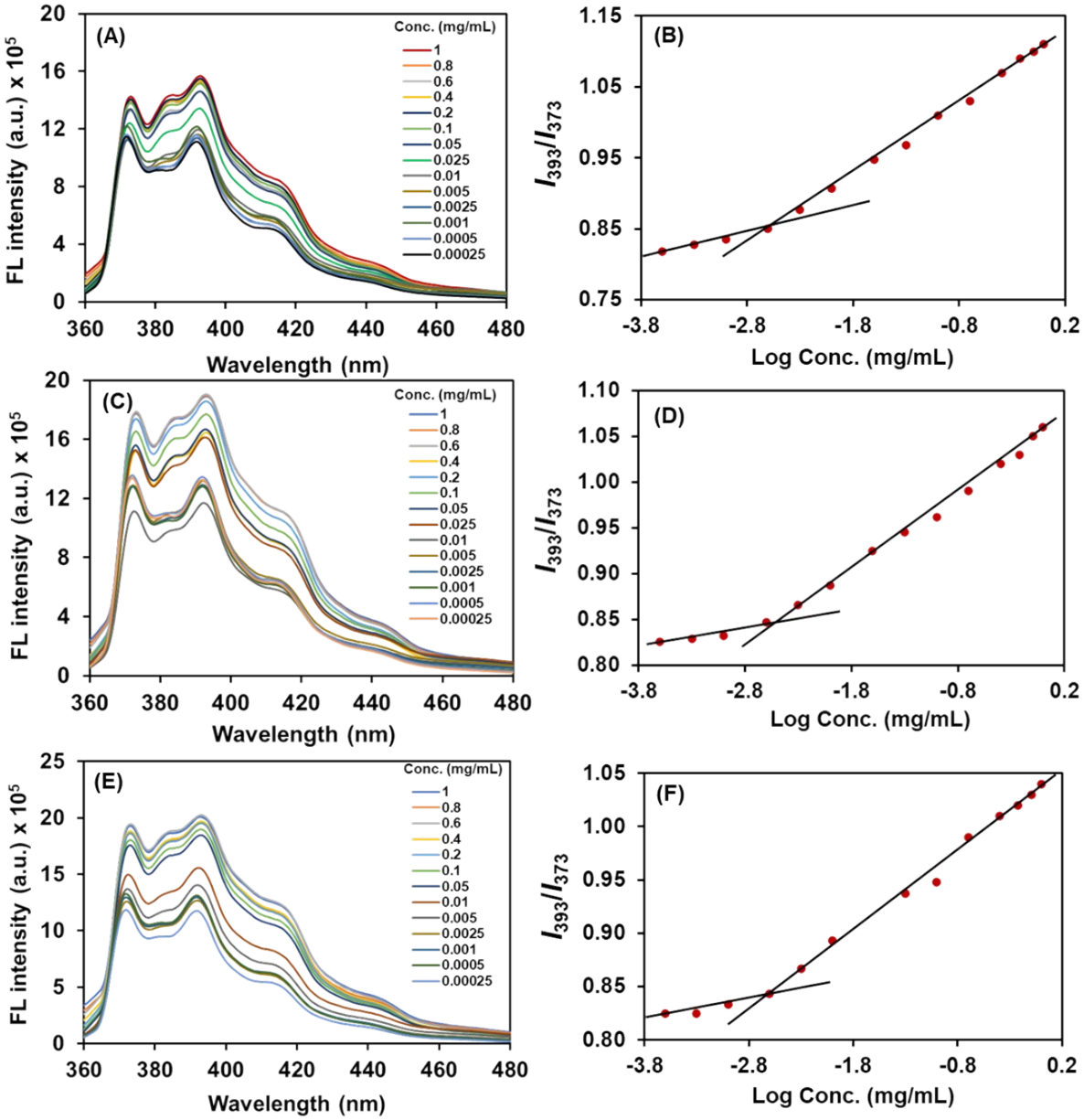

Fig. S4 Fluorescence emission spectra of pyrene at different concentrations of PPEGMA$_{300}$-*b*-PMAMA (image A), PPEGMA$_{300}$-*b*-PPAMA (image C), and PPEGMA$_{300}$-*b*-PSAMA (image E) in water, and plot of intensity ratio I_{393}/I_{373} versus logarithm of concentrations of PPEGMA$_{300}$-*b*-PMAMA (image B), PPEGMA$_{300}$-*b*-PPAMA (image D) and PPEGMA$_{300}$-*b*-PSAMA (image F).

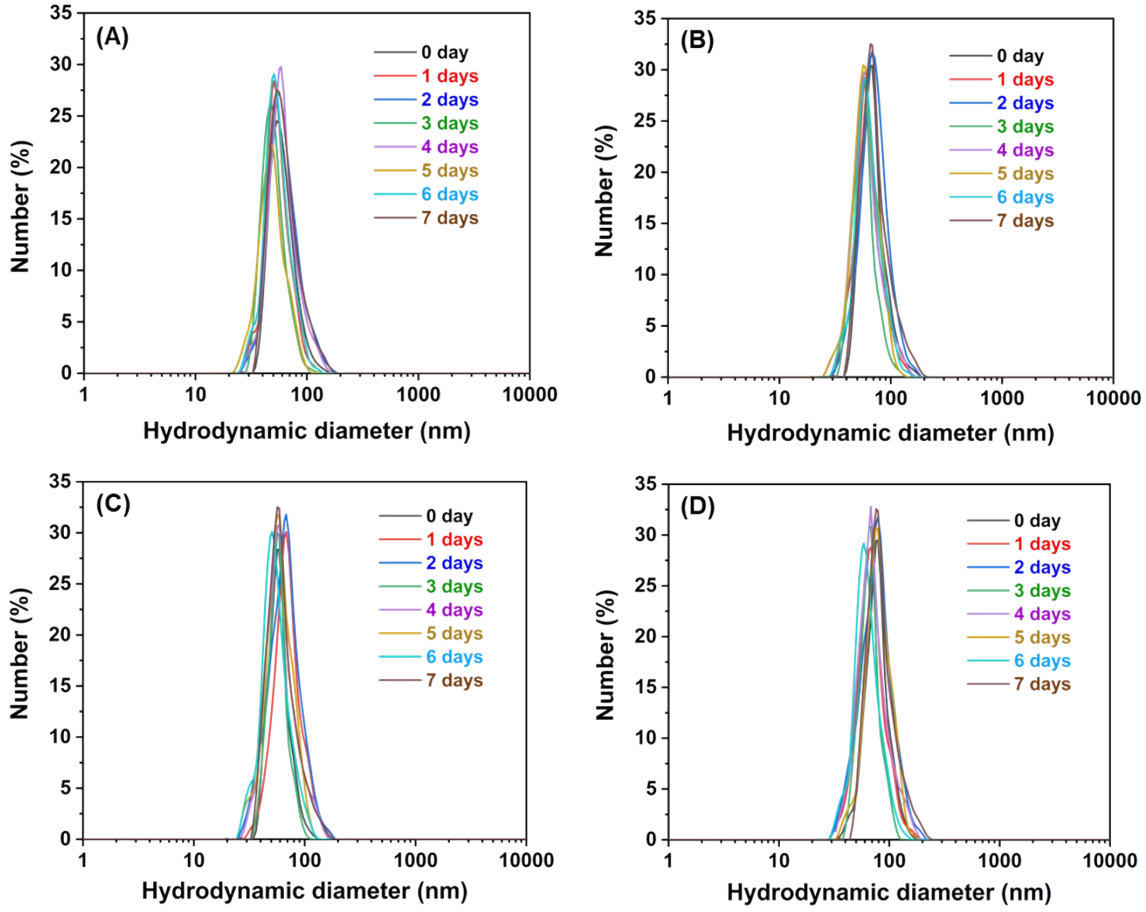

Fig. S5 Size distribution profile of (A) PPEGMA$_{300}$-*b*-PLAMA, (B) PPEGMA$_{300}$-*b*-PMAMA, (C) PPEGMA$_{300}$-*b*-PPAMA and (D) PPEGMA$_{300}$-*b*-PSAMA micelles over a period of 7 days.

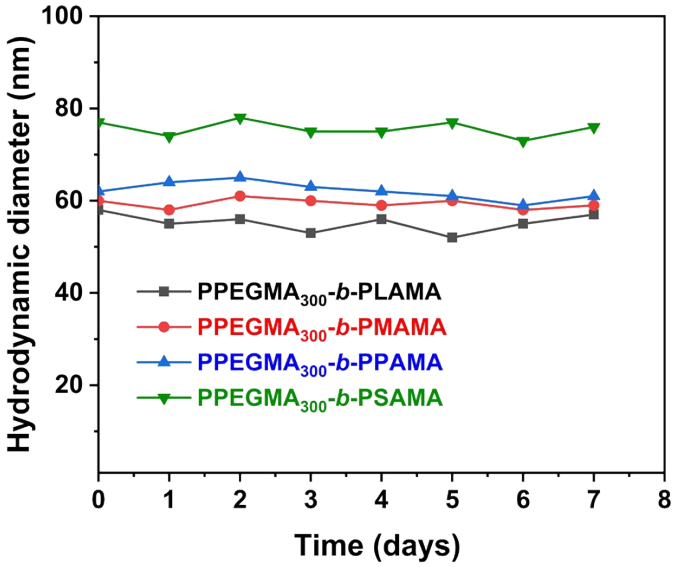

Fig. S6 Stability study of polymeric micelles over a period of 7 days.

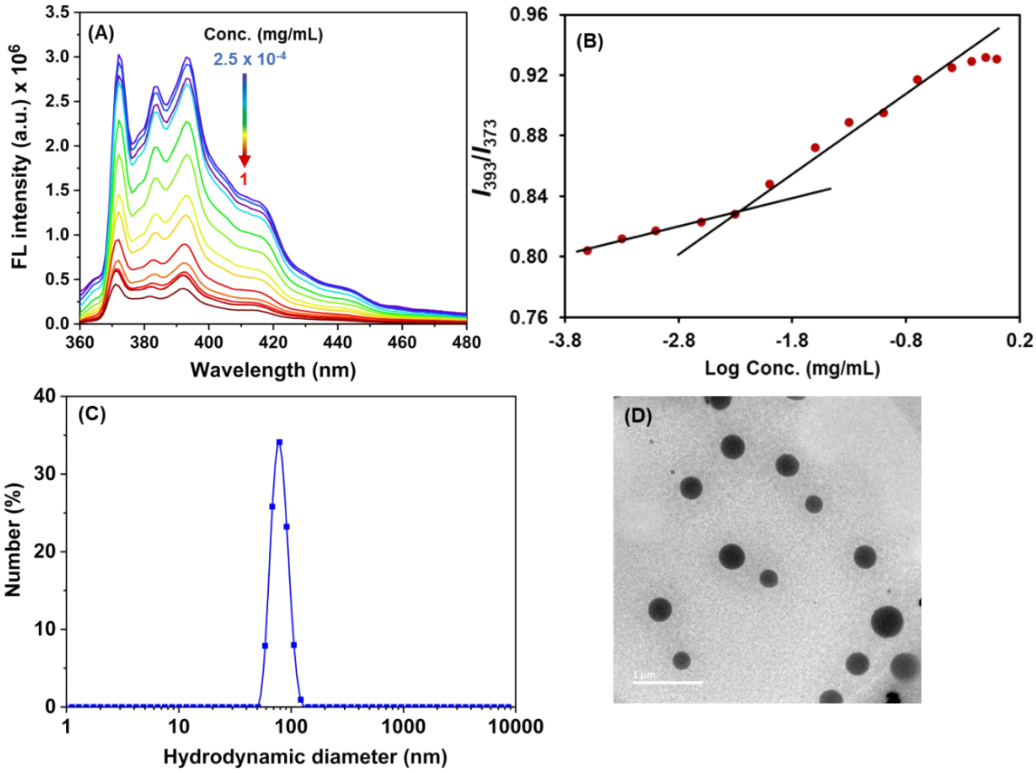

Fig. S7 (A) Fluorescence emission spectra of pyrene at different concentrations of PPEGMA$_{475}$-*b*-PSAMA in water, (B) Plot of intensity ratio I_{393}/I_{373} versus logarithm of concentrations of PPEGMA$_{475}$-*b*-PSAMA, (C) Size distribution profile, and (D) TEM image (Scale bar = 1 μm) of PPEGMA$_{475}$-*b*-PSAMA micelles in water.

Table S1. Lag phase time obtained by fitting the kinetic data and the inhibitory rate of different **FABC** micelles against the insulin fibrillation process.

Sample type	Lag phase (min)	Inhibitory rate (%)
Insulin Fibrils	84	-
Insulin Fibrils+**LABCP$_{300}$**	122	81±2.0
Insulin Fibrils+**MABCP$_{300}$**	117	83±3.0
Insulin Fibrils+**PABCP$_{300}$**	104	84±2.5
Insulin Fibrils+**SABCP$_{300}$**	88	88±1.5
Insulin Fibrils+**SABCP$_{475}$**	156	95±2.0

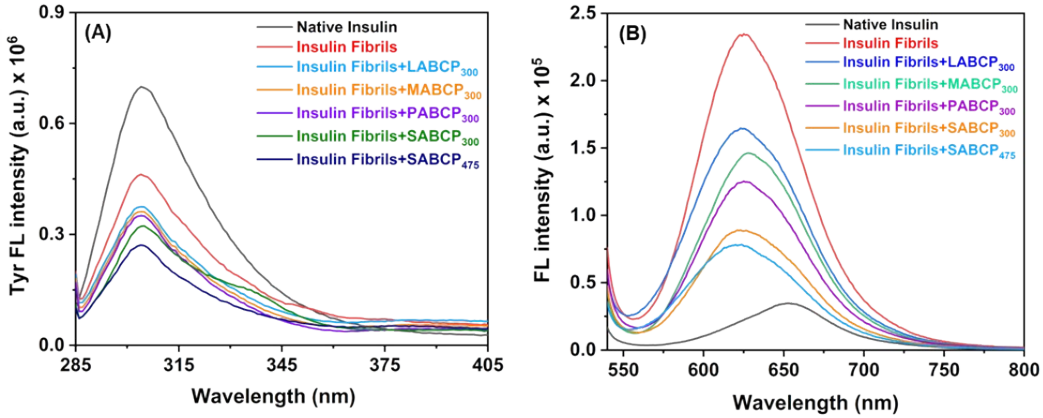

Fig. S8 (A) Tyr fluorescence spectra (λ_{ex} = 276 nm); (B) Nile red fluorescence spectra (λ_{ex} = 530 nm) of insulin fibrils incubated alone and in the presence of different **FABC** micelles. Sample concentration was fixed at 5 μM for Tyr fluorescence spectra and for NR fluorescence spectra the sample and NR concentration were maintained at 2.5 and 10 μM, respectively.

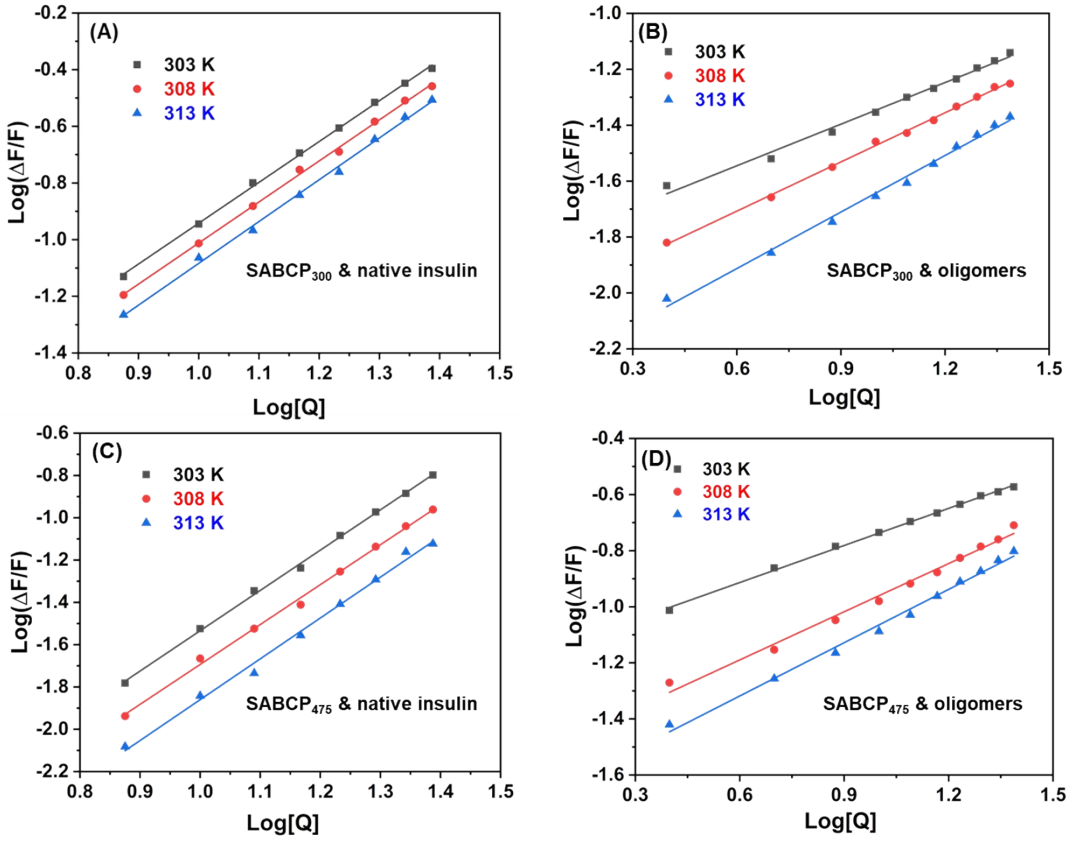

Fig. S9 Representative double logarithm plots for the interaction of (A) **SABCP$_{300}$** micelles with native insulin; (B) **SABCP$_{300}$** micelles with insulin oligomers; (C) **SABCP$_{475}$** micelles with native insulin; and (D) **SABCP$_{475}$** micelles with insulin oligomers at 303 K, 308 K, and 313 K temperature.

Table S2. Thermodynamic parameters for the interactions of insulin monomer/oligomers with **SABCP$_{300}$** and **SABCP$_{475}$** micelles.

System	Temperature (K)	ΔG^0 (KJ/mol)	ΔH^0 (KJ/mol)	ΔS^0 (J/mol K)
SABCP$_{300}$-native insulin	303 308 313	-17.1 -16.9 -16.7	-27.8	-35.3
SABCP$_{300}$-insulin oligomers	303 308 313	-50.2 -49.8 -49.4	-74.5	-80.2
SABCP$_{475}$-native insulin	303 308 313	-33.4 -33.1 -32.8	-49.4	-53.0
SABCP$_{475}$-insulin oligomers	303 308 313	-87.1 -86.5 -85.8	-128.1	-135.2

Table S3. Lifetime decay data of DCM dye in native insulin, IF, and IF in the presence of **FABC** micelles by fitting the data using the IBH DAS6 (version 2.2) software.

Sample set	τ_1 (ns)	B_1	τ_2 (ns)	B_2	τ_3 (ns)	B_3	$\langle\tau\rangle$ (ns)	χ^2
DCM dye	0.13	53	1.01	46	-	-	0.89	1.12
Native insulin	0.14	59	0.98	57	-	-	0.87	1.08
IF	1.98	35	0.05	2	4.01	66	3.58	1.10
IF + L**ABCP$_{300}$**	1.80	32	3.52	74	0.41	2	3.20	1.07
IF + M**ABCP$_{300}$**	1.67	29	3.47	69	0.23	2	3.16	1.05
IF + P**ABCP$_{300}$**	1.58	22	3.39	65	0.24	2	3.13	1.10
IF + **SABCP$_{300}$**	1.38	6	2.30	90	0.18	2	2.26	1.13
IF + S**ABCP$_{475}$**	1.06	15	1.90	63	0.23	3	1.79	1.06

Table S4. Hydrodynamic diameters of insulin fibrils in the presence and absence of **FABC** micelles.

Sample type	Hydrodynamic diameter (nm)
Native Insulin	5±2.0
Insulin Fibrils	700±12.0
Insulin Fibrils + **LABCP$_{300}$**	91±3.0
Insulin Fibrils + **MABCP$_{300}$**	68±4.5
Insulin Fibrils + **PABCP$_{300}$**	59±1.2
Insulin Fibrils + **SABCP$_{300}$**	50±2.7
Insulin Fibrils + **SABCP$_{475}$**	43±3.8

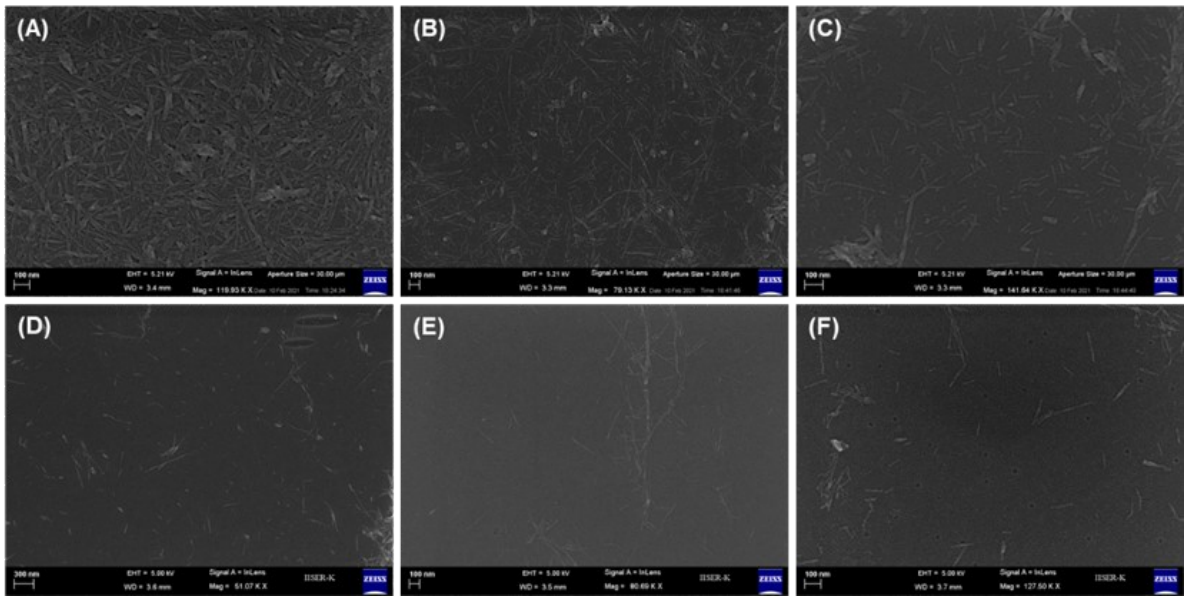

Fig. S10 FESEM images of (A) insulin fibrils, (B)-(F) IF in the presence of **LABCP$_{300}$**, **MABCP$_{300}$**, **PABCP$_{300}$**, **SABCP$_{300}$**, and **SABCP$_{475}$** micelles respectively obtained upon incubation of the samples for a period of 24 h at 65 °C.

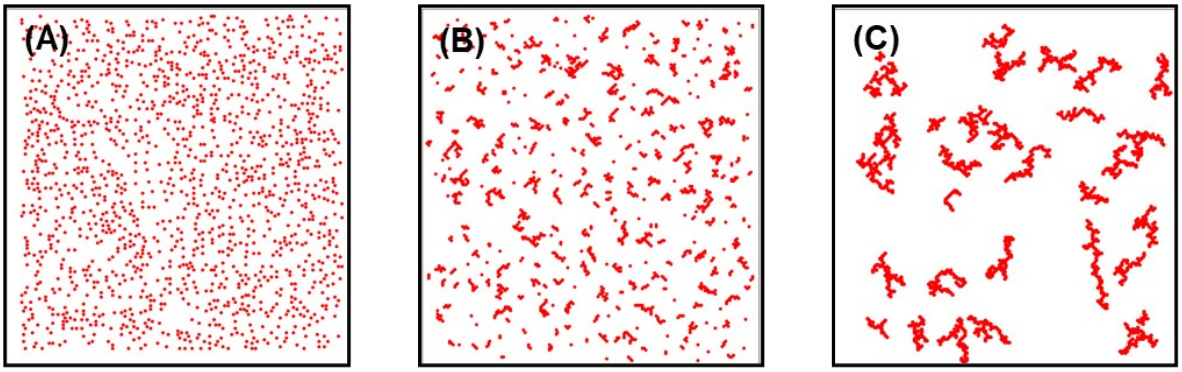

Fig. S11 Time evolution of insulin fibrillation process in the absence of **FABC** micelles. (A) Initially, N = 1500 monomers are randomly deposited on (200 × 200) lattice system. (B) As time progresses, diffusing monomers stick together to form oligomers and larger aggregates. (C) After sufficiently long-time matured fibrils are formed.

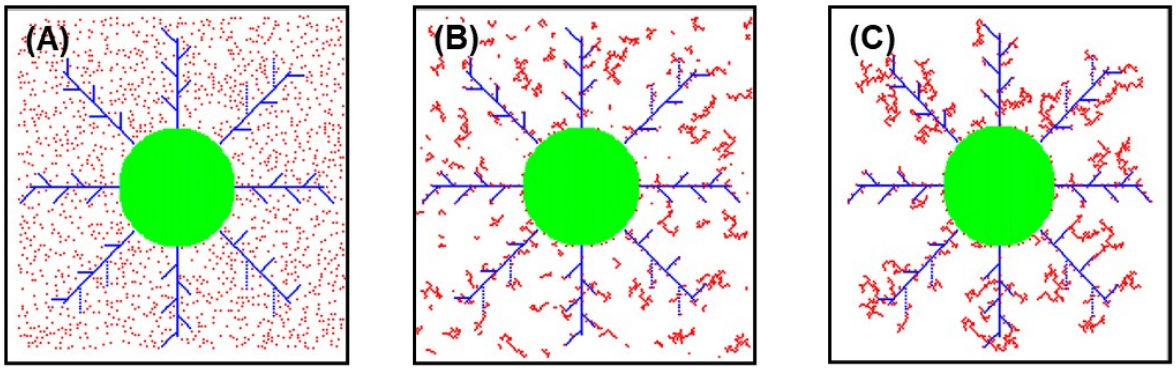

Fig. S12 Time evolution of insulin fibrillation process in the presence of **LABCP$_{300}$** micelle. (A) Initially, N = 1500 monomers are randomly deposited on (200 × 200) lattice system around the micelle. (B) As time progresses, monomers start to diffuse, come in frequent contact with the micelle structure, and stick to the micelle preventing the insulin fibrillation process. (C) Eventually, all monomers, oligomers, and protofibrils get stick to the micelle, and it hinders the formation of long matured fibrils. The average size of the aggregates becomes much smaller compared to the long fibril formation in the absence of micelle.

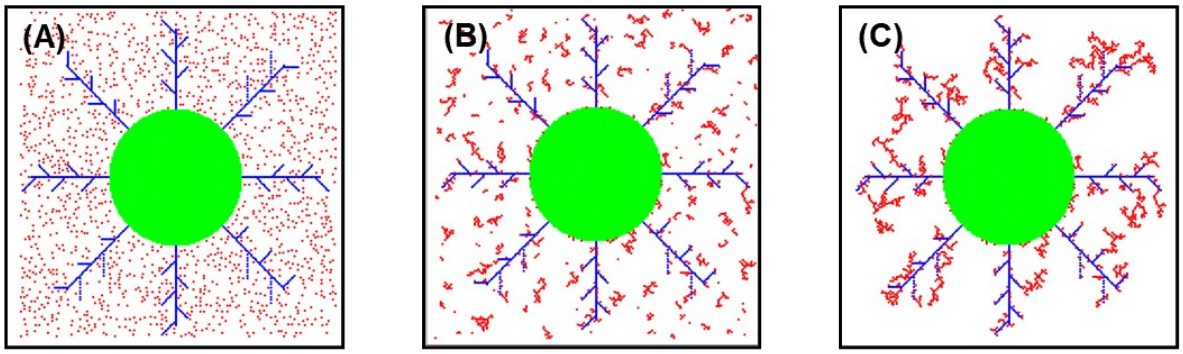

Fig. S13 Time evolution of insulin fibrillation process in the presence of **SABCP$_{300}$** micelle. (A) Initially, $N = 1500$ monomers are randomly deposited on (200 × 200) lattice system around the micelle. (B) As time progresses, monomers start to diffuse, collide and stick to the micelles. As the core diameter of the micelle is increased by 20%, diffusing monomers get a larger area to attach to the micelle. (C) Finally, all monomers, oligomers, and protofibrils get stick to the micelle, and it hinders the formation of long matured fibrils. The average size of the aggregates is smaller in the system compared to **LABCP$_{300}$**.

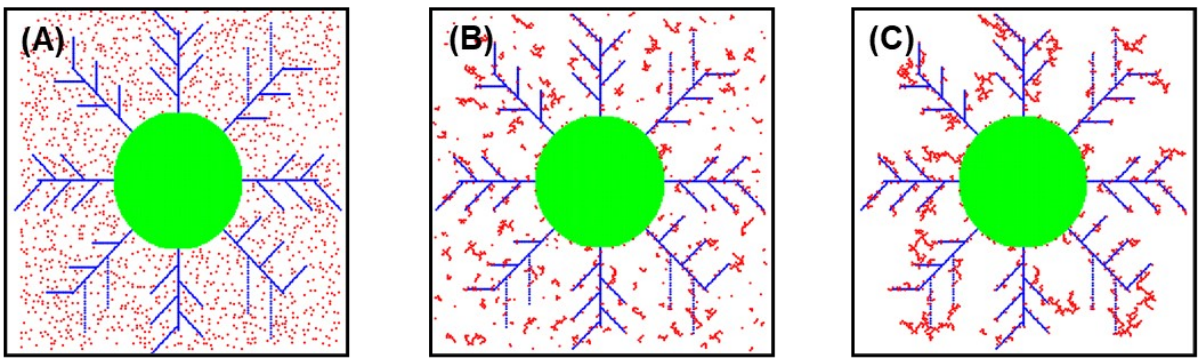

Fig. S14 Time evolution of insulin fibrillation process in the presence of **SABCP$_{475}$** micelles. (A) Initially, $N = 1500$ monomers are randomly deposited on (200 × 200) lattice system around the micelle. (B) As time progresses, insulin monomers start to diffuse, collide and stick to the longer side chains on the outer shell of the micelle preventing significantly the insulin fibrillation process. (C) Eventually, all monomers and oligomers stick to the micelle. The average size of the aggregates becomes very small, showing that **SABCP$_{475}$** can successfully inhibit the formation of matured fibrils.

References

(1) P. Ghosh, A. Bera, A. Ghosh, P. Bhadury and P. De, *ACS Appl. Bio Mater.*, 2020, **3**, 5407-5419.

(2) B. Lu, Y. Li, Z. Wang, B. Wang, X. Pan, W. Zhao, X. Ma and J. Zhang, *New J. Chem*., 2019, **43**, 12275-12282.

(3) K. G. Goswami, S. Mete, S. Som Chaudhury, P. Sar, E. Ksendzov, C. Das Mukhopadhyay, S. V. Kostjuk and P. De, *ACS Appl. Polym. Mater*., 2020, **2**, 2035-2045.

(4) A. S. Hudson, H. Ecroyd, W. T. Kee and A. J. Carver, *FEBS Journal*, 2009, **276**, 5960-5972.

(5) Y. M. Kwon, M. Baudys, K. Knutson and S. W. Kimet, *Pharm. Res.*, 2001, **18**, 1754-1759.

(6) P. Paul, M. Karar, A. Mallick and T. Majumdar, *J. Mater. Chem. C*, 2021, **9**, 11229-11241.

(7) C. R. Cantor and P. R. Schimmel, Biophysical Chemistry W. H. Freeman and Company, Eleventh Edition: New York, 2004.

(8) H. Gong, Z. He, A. Peng, X. Zhang, B. Cheng, Y. Sun, L. Zheng and K. Huang, *Sci. Rep*., 2014, **4**, 5648-5655.

(9) K. H. Yu and C. I. Lee, *Pharmaceutics*, 2020, **12**, 1081-1090.